

# Subspace Variational Quantum Simulator

Kentaro Heya,<sup>1,\*</sup> Ken M. Nakanishi,<sup>2,†</sup> Kosuke Mitarai,<sup>3,4,‡</sup> and Keisuke Fujii<sup>3,5,§</sup>

<sup>1</sup>*Research Center for Advanced Science and Technology (RCAST),  
The University of Tokyo, Meguro-ku, Tokyo 153-8904, Japan*

<sup>2</sup>*Graduate School of Science, The University of Tokyo,  
7-3-1 Hongo, Bunkyo-ku, Tokyo 113-0033, Japan.*

<sup>3</sup>*Graduate School of Engineering Science, Osaka University,  
1-3 Machikaneyama, Toyonaka, Osaka 560-8531, Japan.*

<sup>4</sup>*QunaSys Inc., High-tech Hongo Building 1F, 5-25-18 Hongo, Bunkyo, Tokyo 113-0033, Japan.*

<sup>5</sup>*JST, PRESTO, 4-1-8 Honcho, Kawaguchi, Saitama 332-0012, Japan*

(Dated: April 19, 2019)

Quantum simulation is one of the key applications of quantum computing [1], which can accelerate research and development in chemistry, material science, etc. Here, we propose an efficient method to simulate the time evolution driven by a static Hamiltonian, named subspace variational quantum simulator (SVQS). SVQS employs the subspace-search variational eigensolver (SSVQE) [2] to find a low-energy subspace and further extends it to simulate dynamics within the low-energy subspace. More precisely, using a parameterized quantum circuit, the low-energy subspace of interest is encoded into a computational subspace spanned by a set of computational basis, where information processing can be easily done. After the information processing, the computational subspace is decoded to the original low-energy subspace. This allows us to simulate the dynamics of low-energy subspace with lower overhead compared to existing schemes. While the dimension is restricted for feasibility on near-term quantum devices, the idea is similar to quantum phase estimation and its applications such as quantum linear system solver and quantum metropolis sampling. Because of this simplicity, we can successfully demonstrate the proposed method on the actual quantum device using Regetti Quantum Cloud Service. Furthermore, we propose a variational initial state preparation for SVQS, where the initial states are searched from the simulatable eigensubspace. Finally, we demonstrate SVQS on Rigetti Quantum Cloud Service.

## I. INTRODUCTION

We are now in the era of noisy intermediate-scale quantum (NISQ) devices [3]. A NISQ device is a controllable quantum system, which still has a non-negligible amount of errors in its operation. However, it is believed that such a quantum device with a sufficient number of qubits and a low-enough error rate is not simulatable on classical computers [4–6]. In this sense, NISQ devices might have higher computational power than a classical computer. Especially, we believe that they are likely to be advantageous in preparing a quantum state of interest or simulating a time evolution of a quantum system.

For such an application of NISQ devices, the variational quantum eigensolver (VQE) [7–10] has recently attracted much attention. The VQE was proposed originally as an algorithm to find the ground state of a given Hamiltonian  $\mathcal{H}$ . There, we use a parametrized quantum circuit  $U(\boldsymbol{\theta})$  and optimize the parameter  $\boldsymbol{\theta}$  to minimize an expectation value of the Hamiltonian  $\langle \mathcal{H} \rangle = \langle \psi(\boldsymbol{\theta}) | \mathcal{H} | \psi(\boldsymbol{\theta}) \rangle$ , where  $|\psi(\boldsymbol{\theta})\rangle$  is an ansatz state obtained by applying the circuit  $U(\boldsymbol{\theta})$  to an input state  $|\varphi_{\text{in}}\rangle$ . Successfully optimizing the appropriate param-

eterized quantum circuit, we can get the ground state of the Hamiltonian as the output of the circuit.

The dynamics of quantum systems can exhibit interesting phenomena such as dynamical quantum phase transition [11] or discrete time crystals [12, 13], which are yet to be fully understood. Furthermore, dynamical properties of quantum systems are practically important, and hence researchers have used methods like the time-dependent density functional theory [14]. As Feynman stated [15], a controllable quantum system must be advantageous in simulating such dynamics over a classical computer.

As for the simulation of the time evolution of a quantum system, Ref. [1] has proposed a variational quantum simulator (VQS), which simulates the time evolution of quantum states under a given Hamiltonian  $\mathcal{H}$ . In the VQS, time-dependent parameter  $\boldsymbol{\theta}(t + \delta t)$  is utilized as the parameter of the quantum circuit. The algorithm determines the parameter  $\boldsymbol{\theta}(t + \delta t)$  by minimizing the difference between the actual time-evolved state  $e^{-i\mathcal{H}\delta t} |\psi(\boldsymbol{\theta}(t))\rangle$  and  $|\psi(\boldsymbol{\theta}(t + \delta t))\rangle$ . For this minimization, one measures the gradient of energy expectation value  $\mathbf{V} = \left\{ \left( \frac{\partial \langle \mathcal{H}(\boldsymbol{\theta}) \rangle}{\partial \theta_i} \right) \right\}$  and the imaginary part of the metric tensor  $M = \left\{ \text{Im} \left( \frac{\partial \langle \psi(\boldsymbol{\theta}) |}{\partial \theta_i} \frac{\partial |\psi(\boldsymbol{\theta}) \rangle}{\partial \theta_j} \right) \right\}$ . With these,  $\boldsymbol{\theta}(t + \delta t)$  is calculated according to the differential equation  $M \frac{d\boldsymbol{\theta}(t)}{dt} = \mathbf{V}$ . This method is a pioneering work for performing a quantum simulation without Trotterization on NISQ devices.

In this paper, we propose another approach to simulate

\* kheyaa@qc.rcast.u-tokyo.ac.jp

† ken-nakanishi@g.ecc.u-tokyo.ac.jp

‡ mitarai@qc.ee.es.osaka-u.ac.jp

§ fujii@qc.ee.es.osaka-u.ac.jp

a time evolution of a quantum system, which we call the subspace variational quantum simulation (SVQS), and demonstrate proof-of-principle experiments on Rigetti Quantum Cloud Service. The SVQS simulates dynamics that evolve in a space spanned by the low-lying excited states and the ground state. This is based on our recent work, subspace-search variational quantum eigensolver (SSVQE) [2], which is an extension of the VQE to a subspace search problem. Our algorithm works as follows. First, we run SSVQE to find a unitary  $U(\boldsymbol{\theta}^*)$  that maps  $k$  orthogonal input states  $\{|\varphi_i\rangle\}_{i=1}^k$ , which we choose from computational basis, to the excited states up to the  $k$ -th,  $\{|E_i\rangle\}_{i=1}^k$  of  $\mathcal{H}$ , each having the corresponding eigenenergy  $E_i$ . Note that the inverse of the unitary,  $U^\dagger(\boldsymbol{\theta}^*)$ , maps each  $|E_i\rangle$  to computational basis  $|\varphi_i\rangle$ , where we can easily apply phase factors  $e^{iE_it}$ . Therefore, we can perform the simulation of  $e^{-i\mathcal{H}t}$  by applying  $U^\dagger(\boldsymbol{\theta}^*)$  to an input state  $|\psi_{\text{in}}\rangle \in \text{span}\{|E_i\rangle\}_{i=1}^k$ , then applying the phase, and finally applying  $U(\boldsymbol{\theta}^*)$  to return the state to its initial basis.

Our protocol does not require the gradient or the metric tensor for simulation. The only thing we have to do is to find the unitary  $U(\boldsymbol{\theta}^*)$  that transforms the low energy subspace to a subspace spanned by computational basis. The simplicity of our protocol enables us to do the simulation with lower overhead than the VQS. Moreover, we do not need to discretize the simulation by a small timestep  $\delta t$ , that is, we can perform the simulation of an arbitrary time duration without increasing the depth of the circuit. Although the simulation is restricted into space spanned by the low-lying states in the proposed method, they are often the states of the interest. We successfully demonstrate the proof-of-principle experiments of our method on Rigetti's superconducting quantum computer. In the experiments, we employ error-mitigation techniques [1, 16, 17] to observe quantum dynamics accurately even in the presence of noise.

This work presents an efficient algorithm to simulate the quantum dynamics on a NISQ device. While the dimension of the simulatable subspace is limited, this algorithm shares the idea with the long-term quantum algorithms based on quantum phase estimation such as Harrow-Hassidim-Lloyd algorithm [18] for solving linear problem and the quantum recommendation systems [19]. More precisely, both approaches transform the input state to another basis on which we can manipulate their eigenvalues easily and then undo the basis change. From this respect, the SSVQE and the SVQS can be regarded as a NISQ version of quantum phase estimation and its application, respectively. This correspondence might provide a deeper insight into the relationship between the near-term quantum algorithms and long-term quantum algorithms.

## II. METHODS

In this section, we first introduce the subspace-search variational quantum eigensolver (SSVQE) [2], which is the key ingredient for our proposed method. We then describe our proposal, the subspace variational quantum simulator (SVQS). In the following subsections,  $\mathcal{H}$  denotes a given  $n$ -qubit target Hamiltonian, which can be written as follows,

$$\mathcal{H} = \sum_{j=1}^{2^n} E_j |E_j\rangle \langle E_j|, \quad (1)$$

where  $E_j$  and  $|E_j\rangle$  are  $j$ -th eigenenergy and eigenstate of  $\mathcal{H}$ , respectively. In application for quantum chemistry, Jordan-Wigner or Bravyi-Kitaev transformation can be utilized to map a fermionic Hamiltonian to an  $n$ -qubit Hamiltonian.

### A. Subspace-search variational quantum eigensolver

The SSVQE is an algorithm for finding the  $k$ -th or up to the  $k$ -th excited states of Hamiltonian  $\mathcal{H}$ . To find excited states up to the  $k$ -th, the SSVQE takes  $k$  orthogonal states as inputs of a parametrized quantum circuit and minimizes the weighted sum of the expected values of the energies of the output states. The output states are automatically orthogonal by the conservation of orthogonality under the unitary transformation, and therefore we are able to find all excited states up to the  $k$ -th by only one optimization procedure. A more detailed explanation is found in Ref. [2]. The procedure of the SSVQE is summarized as follows:

1. Construct a parameterized quantum circuit  $U(\boldsymbol{\theta})$  and prepare  $k$  initial states  $\{|\varphi_j\rangle\}_{j=0}^k$  ( $k \leq n$ ), which are orthogonal with each other ( $\langle \varphi_i | \varphi_j \rangle = \delta_{i,j}$ ).
2. Minimize  $\mathcal{L}_\omega(\boldsymbol{\theta}) = \sum_{j=0}^k \omega_j \langle \varphi_j | U^\dagger(\boldsymbol{\theta}) \mathcal{H} U(\boldsymbol{\theta}) | \varphi_j \rangle$ , where the weight vector  $\boldsymbol{\omega}$  is chosen such that  $\omega_i > \omega_j$  when  $i < j$ .

Successfully optimizing  $\boldsymbol{\theta}$  of the appropriate parameterized quantum circuit  $U(\boldsymbol{\theta})$  by the above procedure, each output state  $|\psi_j(\boldsymbol{\theta}^*)\rangle \equiv U(\boldsymbol{\theta}^*) |\varphi_j\rangle$  ( $j = 0, 1, \dots, k$ ) converges to the following state

$$|\psi_j(\boldsymbol{\theta}^*)\rangle = e^{i\delta_j} |E_j\rangle, \quad (2)$$

where  $\delta_j$  is an unknown global phase factor, and  $\boldsymbol{\theta}^*$  denotes the parameters theta that minimizes  $\mathcal{L}_\omega(\boldsymbol{\theta})$ . Therefore, the obtained circuit  $U(\boldsymbol{\theta}^*)$  corresponds to a map between the computational subspace  $S_{\text{com}}$  formed by the orthogonal initial states  $\{|\varphi_j\rangle\}_{j=1}^k$  and the eigensubspace  $S_{\text{eig}}$  formed by the excited states  $\{|E_j\rangle\}_{j=1}^k$ . While the

above unknown global phase factors are thought to cause a problem to prepare a desired superposition of the energy eigenstate, this is not the case as we will see later.

## B. Subspace variational quantum simulator

In this subsection, we describe our proposal, which we name the subspace variational quantum simulator (SVQS). The key idea of the SVQS is mapping low-energy eigensubspace  $\mathcal{S}_{\text{eig}}$  of the target Hamiltonian  $\mathcal{H}$  to subspace  $\mathcal{S}_{\text{com}}$  spanned by computational basis which can be controlled easily. The procedure of the SVQS is summarized as follows:

1. Construct a parameterized quantum circuit  $U(\boldsymbol{\theta})$  and prepare  $l$  input states  $\{|\varphi_j\rangle\}_{j=1}^l$  ( $l \leq n$ ) such that they are orthogonal with each other ( $\langle\varphi_j|\varphi_{j'}\rangle = \delta_{j,j'}$ ).
2. Minimize  $\mathcal{L}_\omega(\boldsymbol{\theta}) = \sum_{j=1}^l \omega_j \langle\varphi_j|U^\dagger(\boldsymbol{\theta})\mathcal{H}U(\boldsymbol{\theta})|\varphi_j\rangle$ , where the weight vector  $\boldsymbol{\omega}$  is chosen such that  $\omega_i > \omega_j$  when  $i > j$ . Hereafter,  $\boldsymbol{\theta}^* = \arg \min \mathcal{L}_\omega(\boldsymbol{\theta})$ .
3. Prepare an initial state  $|\psi_{\text{in}}\rangle$  in the eigensubspace  $\mathcal{S}_{\text{eig}}$ .
4. Encoding the input state  $|\psi_{\text{in}}\rangle$  on the eigensubspace  $\mathcal{S}_{\text{eig}}$  into the computational subspace  $\mathcal{S}_{\text{com}}$  by applying the Hermitian conjugate of the obtained circuit  $U^\dagger(\boldsymbol{\theta}^*)$ .
5. Apply single-qubit  $Z$ -rotation on each qubit, namely,  $\mathcal{T}(t) = \bigotimes_{j=1}^l R_Z(-E_j t)$ , where  $\{E_j\}_{j=1}^l$  are the eigenenergies of the eigenstates  $\{|E_j\rangle\}_{j=1}^l$  obtained by SSVQE.
6. Decoding the state  $\mathcal{T}(t)U^\dagger(\boldsymbol{\theta}^*)|\psi_{\text{in}}\rangle$  on the computational subspace  $\mathcal{S}_{\text{com}}$  into the eigensubspace  $\mathcal{S}_{\text{eig}}$  by applying  $U(\boldsymbol{\theta}^*)$ . See also Fig. 1 which is the quantum circuit corresponding to the step 4-6 of the procedure.

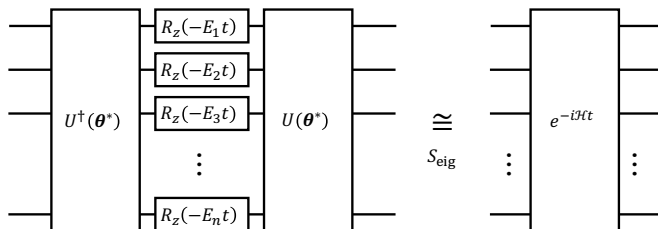


FIG. 1. Quantum circuit for SVQS.  $R_Z(\xi)$  denotes single-qubit  $Z$ -rotation with rotation angle  $\xi$ . The quantum circuit shown on the left approximates the time evolution operator within the eigensubspace  $\mathcal{S}_{\text{eig}}$ .

Let us explain how the above procedure works to simulate the time evolution of the quantum system. The obtained

circuit  $U(\boldsymbol{\theta}^*)$  corresponds to a map between  $\mathcal{S}_{\text{eig}}$  and  $\mathcal{S}_{\text{com}}$ . Therefore, the circuit  $U(\boldsymbol{\theta}^*)$  can be denoted as follows,

$$U(\boldsymbol{\theta}^*) = \sum_j e^{i\delta_j} |E_j\rangle \langle\varphi_j| + U_\perp, \quad (3)$$

where  $\{\delta_j\}_{j=1}^l$  are unknown phase offsets and  $U_\perp$  is an unknown map between subspaces complementary to  $\mathcal{S}_{\text{eig}}$  and  $\mathcal{S}_{\text{com}}$ . The tensor product of single-qubit  $Z$ -rotations can be denoted as follows,

$$\mathcal{T}(t) = \sum_{j=1}^l e^{-iE_j t} |\varphi_j\rangle \langle\varphi_j| + U'_\perp(t), \quad (4)$$

where  $U'_\perp(t)$  is again a map between the complementary subspaces. Under the conjugation by Eq. (3), Eq. (4) transforms as follows:

$$U(\boldsymbol{\theta}^*)\mathcal{T}(t)U^\dagger(\boldsymbol{\theta}^*) = \sum_{j=1}^l e^{-iE_j t} |E_j\rangle \langle E_j| + U_\perp U'_\perp(t) U_\perp^\dagger. \quad (5)$$

Equation (5) corresponds to the time evolution operator on the  $k$ -dimensional eigensubspace with unknown time-dependent unitary operation on the complementary subspace. Note that the number of excited states that we can address here is restricted at most  $n$  because of the construction of the initial orthogonal states by one-hot states  $|\varphi_j\rangle = X_j |0\rangle^{\otimes n}$ .

Note that we here assume that the experimentalist can prepare the initial state  $|\psi_{\text{in}}\rangle$  of his/her interest appropriately without any knowledge about the global phase factors. This assumption would be unlikely, and hence we will relax it in the next subsection.

## C. Variational initial state preparation for SVQS

In Sec. IIB, we assume that the experimentalist can find and prepare the desired initial quantum states in the low-energy eigensubspace  $\mathcal{S}_{\text{eig}}$  which we call a simulatable eigensubspace. However, since there are unknown global phase factors on the obtained energy eigenstates, and hence it is not straightforward for the experimentalist to prepare the desired initial quantum state. In this subsection, we relax this issue by variationally preparing the initial state of interest without any knowledge on the global phase factors.

The dimension of the simulatable eigensubspace  $\mathcal{S}_{\text{eig}}$  in SVQS is restricted by the number of qubits used. Therefore, in general cases, there is no guarantee that the desired initial state is included in the simulatable eigensubspace. Thus, we redefine the initial state preparation as a minimization problem of some cost function  $F(|\psi_{\text{in}}\rangle)$ , which reflects the experimentalist's requests. For example, the cost function can be defined as follows,

$$F(|\psi_{\text{in}}\rangle) = \sum_i (\langle\psi_{\text{in}}|O_i|\psi_{\text{in}}\rangle - O_i^{\text{opt}})^2, \quad (6)$$

where  $O_i$  is some observable, and  $O_i^{\text{opt}}$  is its expectation value that the experimentalist wants. In such cases, the procedure of searching the desired initial quantum states in the simulatable eigensubspace can be further regarded as VQE in the simulatable eigensubspace.

The initial states  $|\psi_{\text{in}}\rangle$  for SVQS are generated by parameterized quantum circuits  $U_{\text{ST}}(\phi)$ . If the parameterized quantum gates closed in the computational subspace  $S_{\text{com}}$ , such as  $R_Z(\theta)$  and  $\exp(-i\theta(|01\rangle\langle 10| + \text{h.c.}))$ , are feasible, the parameterized quantum circuit  $U_{\text{ST}}(\phi)$  can be efficiently composed of them.

After the successful optimization of  $\phi$  to minimize  $F(|\psi_{\text{in}}\rangle)$ , the parameterized initial quantum state converges to the  $|\psi_{\text{in}}(\phi^*)\rangle$ , where  $\phi^*$  denotes the optimal value of  $\phi$ . Then, the time-developed state  $|\psi_{\text{in}}(\phi^*, t)\rangle$  can be written as follows:

$$|\psi_{\text{in}}(\phi^*, t)\rangle = \left\{ U(\theta^*) \bigotimes_{j=1}^l R_Z(-E_j t) \right\} |\psi_{\text{in}}(\phi^*)\rangle. \quad (7)$$

Figure 2 shows the quantum circuit to perform the quantum simulation of the system time evolution.

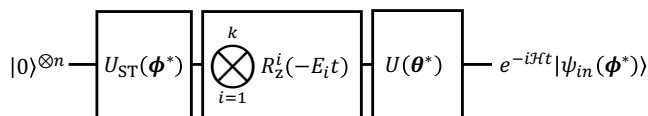


FIG. 2. Quantum circuit for SVQS with variational initial state preparation.

#### D. Extension of simulatable eigensubspace using ancilla qubits

In the methods described in Sec. II B and II C, the dimension of the simulatable eigensubspace  $S_{\text{eig}}$  is limited by  $n$  because of the dimension of the computational subspace. In this section, we propose an additional method to extend the dimension from  $n$  to  $n+a$  by using  $a$  ancilla qubits. The Hamiltonian of the  $(n+a)$ -qubit system is defined in terms of the  $\mathcal{H}_{\text{problem}}$  as follows:

$$\mathcal{H} = \mathcal{H}_{\text{problem}} \otimes I^{\otimes a} + BI^{\otimes n} \otimes \sum_{i=n+1}^{n+a} \bigotimes_{j=1}^a (I - \delta_{i-n,j} Z), \quad (8)$$

where  $I$  and  $Z$  denote the identity and Pauli- $Z$  operator on a single-qubit respectively, and  $B$  is a constant set much larger than the  $(n+a)$ -th excited eigenenergy. The first term of the target Hamiltonian corresponds to

the problem Hamiltonian on the  $n$ -qubit system and the second term of the Hamiltonian corresponds to the static magnetic field  $B$  applied on  $Z$ -axis for the ancilla qubits. If the magnetic field  $B$  is larger than the eigenenergy of the  $(n+a)$ -th excited eigenstate of the problem Hamiltonian, the  $i$ -th excited eigenstate of the target Hamiltonian becomes

$$|\psi_{\text{target}}^i\rangle = |\psi_{\text{problem}}^i\rangle \otimes |0\rangle^{\otimes a}, \quad (9)$$

where  $|\psi_{\text{problem}}^i\rangle$  denote the  $i$ -th excited eigenstate of the problem Hamiltonian. Notice that such a method does not disturb the low-lying eigenstates of the problem Hamiltonian. The  $a$ -ancilla qubits make it possible to use the  $(n+a)$ -orthogonal input states  $\left\{ X_j |0\rangle^{\otimes(n+a)} \right\}_{j=1}^{n+a}$ . This allows us to search up to  $(n+a)$ -th excited states of the  $n$ -qubit Hamiltonian.

### III. EXPERIMENT

Here, we demonstrate our algorithm with 2-qubit experiments on Rigetti Quantum Cloud Service. The ansatz circuit  $U_D(\theta)$ , which we employed in following experiments, consists of  $X$ -rotation  $R_x(\pi/2)$ , parameterized  $Z$ -rotation  $R_z(\theta)$ , and control- $Z$  gate  $CZ$  as shown in Fig. 3.

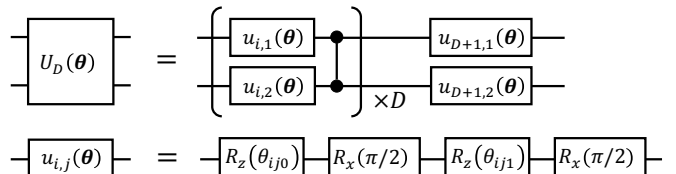


FIG. 3. The ansatz circuit for SSVQE.

Here, we adopt the virtual- $Z$  gate as the parameterized  $Z$ -rotation  $R_z(\theta)$ , whose gate fidelity is known as much higher than other quantum gates,  $R_x(\pi/2)$  and  $CZ$  [20]. The initial values of the parameters are randomly sampled from a uniform distribution  $[0, 2\pi)$ . For the optimization of the parameters in the weighted-SSVQE, we used an optimization method recently reported in Ref. [21]. For the optimization of the parameters of the variational state preparation in the simulatable eigensubspace, we used the BFGS method [22, 23] implemented in the SciPy library [24].

#### A. Single-qubit Rabi oscillation

First, we demonstrate our idea with a single-qubit Rabi oscillation as the simplest quantum dynamic in a two-level system. We consider the Hamiltonian given as follows:

$$\mathcal{H} = \Omega X, \quad (10)$$

where  $\Omega = 0.612$  is a sample from a uniform distribution on  $[0, 1)$ . In this case, the system that we want to simulate is two dimensions, but the dimension of simulatable subspace is one because the system consists of one qubit. Therefore, we employ one ancilla qubit to expand the simulatable subspace from one to two dimensions, which allows us to simulate the Rabi oscillation on a two-level system. An additional Hamiltonian for the ancilla qubit is given as follows:

$$\mathcal{H}' = h(I - Z), \quad (11)$$

where the coefficient  $h = 5$  is selected to be sufficiently larger than the maximum eigenenergy of the system Hamiltonian. The total Hamiltonian becomes

$$\mathcal{H}_{\text{total}} = \mathcal{H} \otimes I + I \otimes \mathcal{H}'. \quad (12)$$

Here, we adopt the ansatz circuit  $U_D(\boldsymbol{\theta})$  with  $D = 1$  as shown in Fig. 3. The optimization process of SSVQE is shown in the appendix. After the convergence of the numerical optimization of the circuit with the weighted-SSVQE on a classical computer, we construct the quantum circuit for the time evolution

$$U_2^\dagger(\boldsymbol{\theta}^*) \bigotimes_{i=1}^n R_Z(\omega_i t) U_2(\boldsymbol{\theta}^*), \quad (13)$$

as shown in Fig. 4

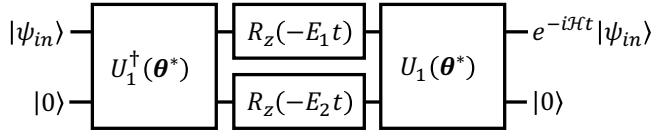


FIG. 4. Quantum circuit for time evolution.

Figure 5 shows the time evolution of the expectation value of the Pauli operators obtained experimentally with  $10^4$  shots.

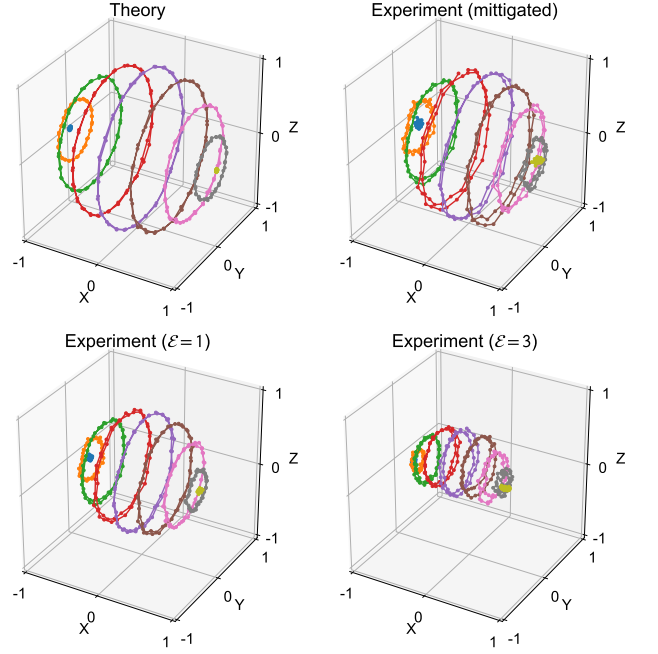


FIG. 5. The expected values of Pauli operators in time-developing quantum states of the data qubit. The colored lines correspond to the initial states of the data qubit given by  $R_Y(i/8\pi)|0\rangle$  with an integer  $i$  ( $-4 \leq i \leq 4$ ). The factor  $\mathcal{E}$  is the error-increased degree for the error mitigation.

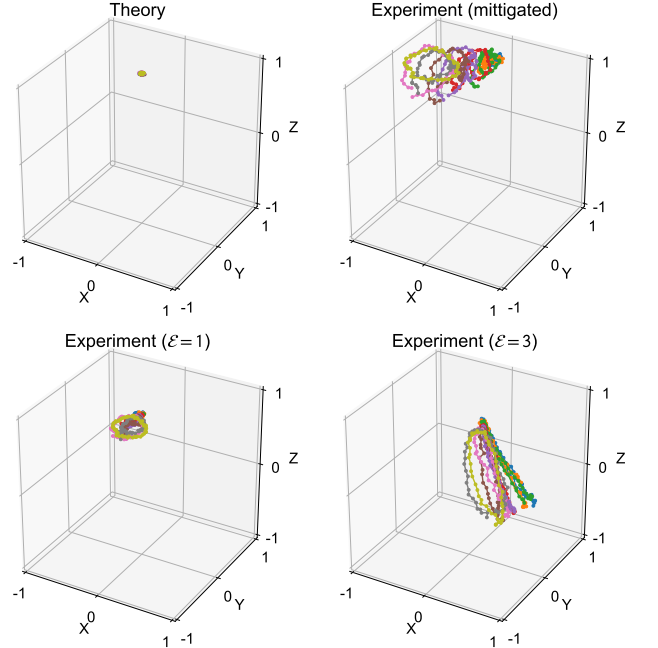


FIG. 6. The expected values of Pauli operators in time-developing quantum states of the ancilla qubit. The colored lines correspond to the initial states of the data qubit given by  $R_Y(i/8\pi)|0\rangle$  with an integer  $i$  ( $-4 \leq i \leq 4$ ). The factor  $\mathcal{E}$  is the error-increased degree for the error mitigation.

Here, we perform the simulation for several initial states

of the data qubit given by  $R_Y(i/8\pi)|0\rangle$  with an integer  $i$  ( $-4 \leq i \leq 4$ ) and the ancilla qubit as  $|0\rangle$ , which are each shown by different colors in Fig. 5.

To obtain an ideal result even in the presence of noise, we use the following error mitigation method [25–27]. Using the result from the error-increased quantum circuits, we apply a linear extrapolation to restore the noiseless data. In order to construct such an error-increased circuit  $U^{(\mathcal{E})}(\boldsymbol{\theta})$ , we replace quantum circuit elements  $R_X(\pi/2)$  and  $CZ$  in  $U(\boldsymbol{\theta})$  with redundant quantum circuit elements  $R_x^{(\mathcal{E})}(\pi/2)$  and  $CZ^{(\mathcal{E})}$  for  $\mathcal{E} \in [1, 3, 5, \dots]$ . They can be denoted as follows,

$$R_x^{(\mathcal{E})}(\pi/2) \equiv R_z(\pi) (R_x(\pi/2))^{\mathcal{E}} R_z(\pi) \quad (14)$$

$$CZ^{(\mathcal{E})} \equiv (CZ)^{\mathcal{E}}. \quad (15)$$

In the ansatz circuit, the fidelity is decreased mainly by  $R_x(\pi/2)$  and  $CZ$  gates. Therefore, the error in  $U^{(\mathcal{E})}(\boldsymbol{\theta})$  is roughly  $\mathcal{E}$ -times larger than that of  $U^{(1)}(\boldsymbol{\theta})$ . From Figs. 5 and 6, one can see that the states of the data qubit rotate in  $X$ -axis and the states of the ancilla qubit stays in  $|0\rangle$  state, which is the behavior expected from the Hamiltonian.

## B. Hydrogen molecule

Next, we demonstrate SVQS with variational initial state preparation for hydrogen molecule using Rigetti QCS. According to Ref. [28], the Hamiltonian of the hydrogen molecule in STO-3G basis can be converted into 2-qubit Hamiltonian as follows,

$$\mathcal{H} = c_0 I + c_1 Z_0 + c_2 Z_1 + c_3 X_0 X_1 + c_4 Y_0 Y_1 + c_5 Z_0 Z_1, \quad (16)$$

where the coefficients  $c_i$  are calculated by openfermion [29] and Psi4 [30]. Here, the occupancy of the coupled and anti-coupled orbital can be calculated from the expectation values of the Pauli operators as follows,

$$n_{\text{coupled}} = \frac{1 - Z_0}{2}, \quad (17)$$

$$n_{\text{anti-coupled}} = \frac{1 - Z_1}{2}. \quad (18)$$

Figure 7 shows the eigenvalue dependence of the Hamiltonian of hydrogen molecules with respect to the interatomic distance.

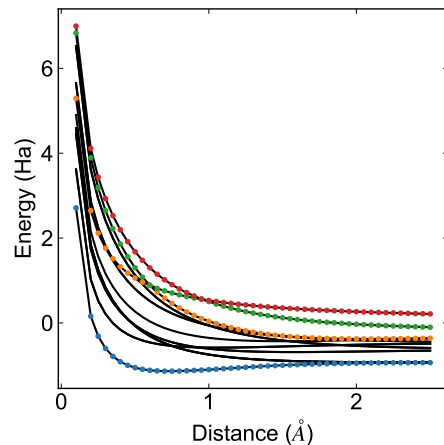


FIG. 7. Eigenvalue dependence of the Hamiltonian of hydrogen molecules with respect to the interatomic distance. The black lines represent the eigenvalues of the Hamiltonian, and the color dots represent the eigenvalues of the reduced Hamiltonian using symmetry [28].

We simulate the dynamics of the Hamiltonians at the interatomic distance  $0.2 \text{ \AA}$  and  $1.0 \text{ \AA}$ . The mapping from the computational subspace to the eigensubspace of the hydrogen molecule is obtained from the numerical calculation of weighted-SSVQE as shown in the appendix. In the weighted-SSVQE, we adopt the ansatz circuit  $U_D(\boldsymbol{\theta})$  with  $D = 2$  as shown in Fig. 3. Next, we prepare the initial quantum state for SVQS. Here, we adopt the cost function for the state preparation as follows,

$$F(|\psi_{\text{in}}(\boldsymbol{\phi})\rangle) = (n_{\text{coupled}} - 0.5)^2 + (n_{\text{anti-coupled}} - 0.5)^2 \quad (19)$$

$$= \frac{\langle Z_0(\boldsymbol{\phi}) \rangle^2 + \langle Z_1(\boldsymbol{\phi}) \rangle^2}{4}, \quad (20)$$

which means that the occupancy of the coupled and anti-coupled orbital need to be close to 0.5 to reduce the cost value. As shown in Figs. 8 and 9, the numerical optimization of the variational state preparation circuit  $U_{\text{ST}}(\boldsymbol{\phi})$ , the cost values converge to 0.249 and 0 when the interatomic distance is  $0.2 \text{ \AA}$  and  $1.0 \text{ \AA}$ , respectively.

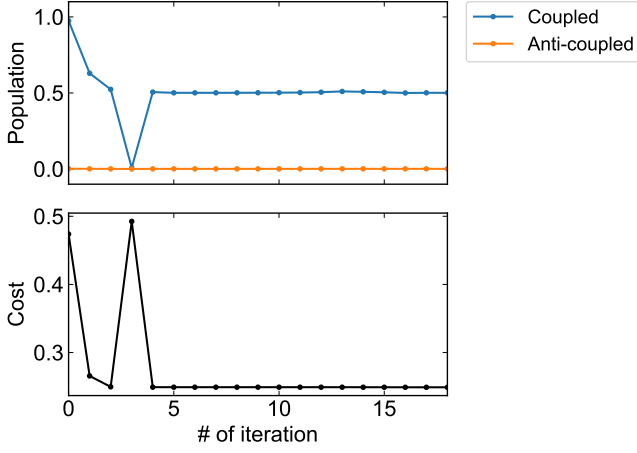


FIG. 8. Numerical optimization of the state preparation circuit  $U_{ST}(\phi)$  with BFGS method. The color lines in the upper drawing represent the occupancies of the coupled and anti-coupled orbitals at each iteration, and the black line in the lower drawing represents the cost function of the optimization at each iteration.

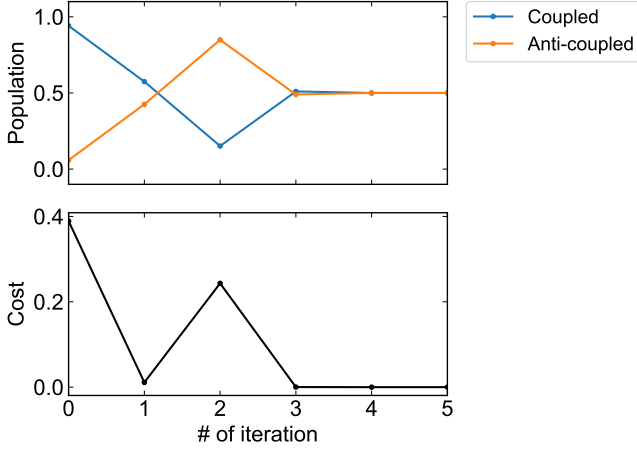


FIG. 9. Numerical optimization of the state preparation circuit  $U_{ST}(\phi)$  with BFGS method. The color lines in the upper drawing represent the occupancies of the coupled and anti-coupled orbitals at each iteration, and the black line in the lower drawing represents the cost function of the optimization at each iteration.

This is because, when the interatomic distance is around  $0.61 \text{ \AA}$ , the first excited state changes, and thus the quantum state included in the eigensubspace formed by the ground and the first excited state changes.

After the convergence of the numerical optimization of the circuit with weighted-SSVQE on a classical computer, we construct the quantum circuit for the simulation of the time evolution of the system as shown in Fig. 10, where  $\theta^*$  and  $\phi^*$  are converged parameters. Figures 11 and 12 shows the actual experimental results of the quantum simulation with  $10^4$  shots.

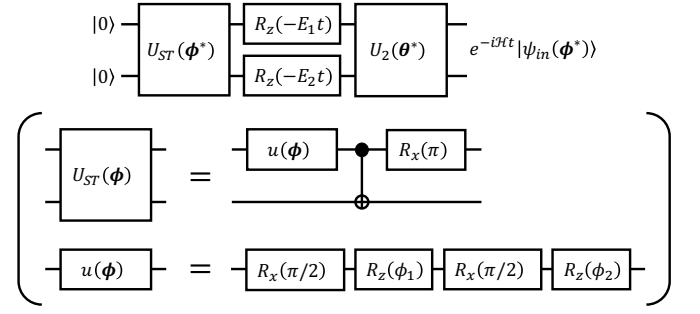


FIG. 10. Quantum circuit for time evolution used to simulate the dynamics of the electrons in the hydrogen molecule.

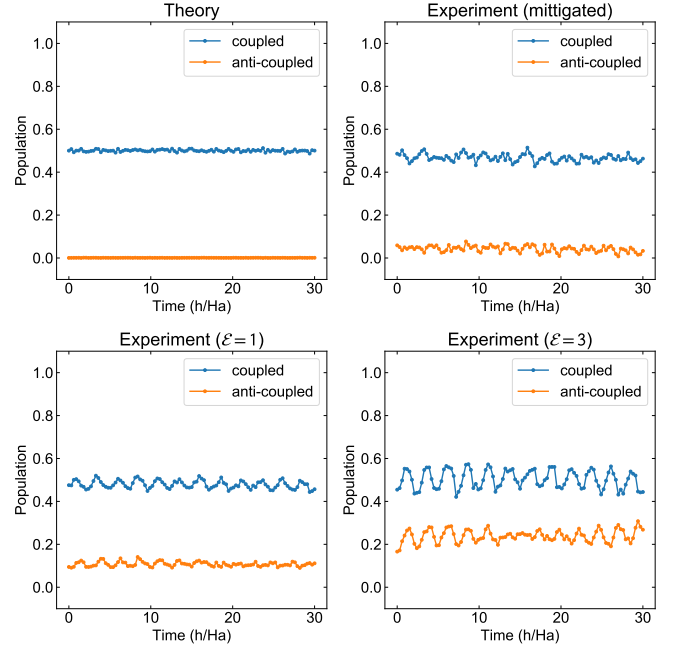


FIG. 11. Temporal evolution of coupled and anti-coupled orbital occupancy in hydrogen molecules with interatomic distance of  $0.2 \text{ \AA}$ . The horizontal axis of the figure corresponds to time, and the unit is  $(\text{h}/\text{Ha})$ , where  $h$  is Planck's constant and  $\text{Ha}$  is Hartley.

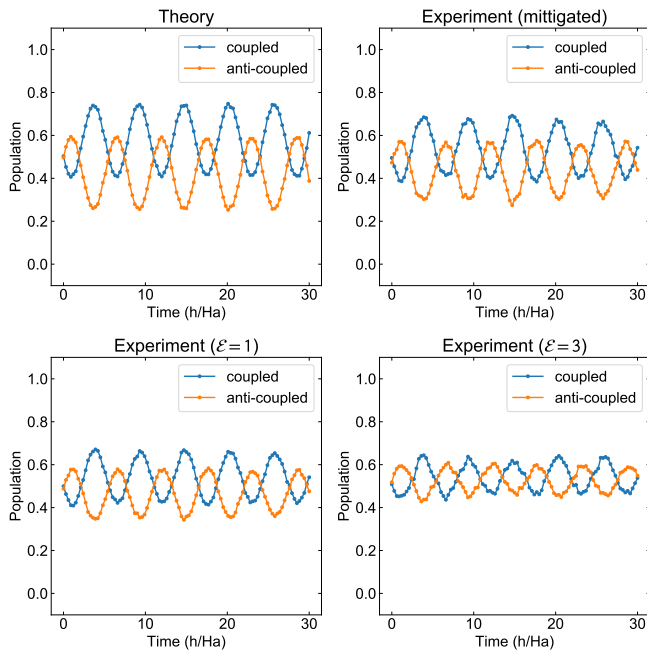


FIG. 12. Temporal evolution of coupled and anti-coupled orbital occupancy in hydrogen molecules with interatomic distance of  $1.0 \text{ \AA}$ . The horizontal axis of the figure corresponds to time, and the unit is  $(h/\text{Ha})$ , where  $h$  is Planck’s constant and  $\text{Ha}$  is Hartley.

From the Figs. 11 and 12, one can see that when the hydrogen atoms are close to each other, the orbital occupancy rate does not change. This is because, when

the interatomic distance is closer, the Hartree-Fock orbitals nicely approximates the eigenstate of the Hamiltonian. On the other hand, When the hydrogen atoms are separated from each other, the orbital occupancy rate changes, because of the poorness of the approximation performed by the Hartree-Fock orbitals.

#### IV. CONCLUSION

We proposed an efficient algorithm to simulate the quantum dynamics on a NISQ device by replacing the QPE with the SSVQE. The circuit depth of the proposed method is at most twice as large as that of VQE. The simplicity of the proposed method enables us to demonstrate it on the existing experimental quantum devices. The proposed method is the first attempt to apply the SSVQE as a near-term version of the QPE, and provides a deeper insight into the relationship between the near-term quantum algorithms and long-term quantum algorithms. For example, it might be able to do more complex processing, such as the HHL algorithm and the simulation of the relaxation process in the low-energy eigensubspace. Also, it would be interesting to do quantum signal processing with simulatable eigensubspace.

#### V. ACKNOWLEDGEMENTS

This work was supported by QunaSys and Rigetti Inc. The numerical simulations were performed with Quantum Toolbox in Python (QuTiP) [31], Open Source Scientific Tools for Python (SciPy) [24], and QuPy [32].

- 
- [1] Y. Li and S. C. Benjamin, *Phys. Rev. X* **7**, 021050 (2017).  
 [2] K. M. Nakanishi, K. Mitarai, and K. Fujii, arXiv preprint arXiv:1810.09434 (2018).  
 [3] J. Preskill, *Quantum* **2**, 79 (2018).  
 [4] S. Boixo, S. V. Isakov, V. N. Smelyanskiy, R. Babbush, N. Ding, Z. Jiang, M. J. Bremner, J. M. Martinis, and H. Neven, *Nat. Phys.* **14**, 595 (2018).  
 [5] A. Bouland, B. Fefferman, C. Nirkhe, and U. Vazirani, arXiv preprint arXiv:1803.04402 (2018).  
 [6] J. Chen, F. Zhang, C. Huang, M. Newman, and Y. Shi, arXiv preprint arXiv:1805.01450 (2018).  
 [7] A. Peruzzo, J. McClean, P. Shadbolt, M. Yung, X. Zhou, P. J. Love, A. Aspuru-Guzik, and J. L. O’Brien, *Nat. Commun.* **5** (2014).  
 [8] J. R. McClean, J. Romero, R. Babbush, and A. Aspuru-Guzik, *New J. Phys.* **18**, 023023 (2016).  
 [9] B. Bauer, D. Wecker, A. J. Millis, M. B. Hastings, and M. Troyer, *Phys. Rev. X* **6**, 031045 (2016).  
 [10] A. Kandala, A. Mezzacapo, K. Temme, M. Takita, M. Brink, J. M. Chow, and J. M. Gambetta, *Nature* **549**, 242 (2017).  
 [11] M. Heyl, *Reports Prog. Phys.* **81**, 054001 (2018).  
 [12] S. Choi, J. Choi, R. Landig, G. Kucsko, H. Zhou, J. Isoya, F. Jelezko, S. Onoda, H. Sumiya, V. Khemani, C. von Keyserling, N. Y. Yao, E. Demler, and M. D. Lukin, *Nature* **543**, 221 (2017).  
 [13] J. Rovny, R. L. Blum, and S. E. Barrett, *Phys. Rev. Lett.* **120**, 180603 (2018).  
 [14] E. Runge and E. K. U. Gross, *Phys. Rev. Lett.* **52**, 997 (1984).  
 [15] R. P. Feynman, *Int. J. Theor. Phys.* **21**, 467 (1982).  
 [16] S. Endo, S. C. Benjamin, and Y. Li, *Phys. Rev. X* **8**, 31027 (2018).  
 [17] K. Temme, S. Bravyi, and J. M. Gambetta, *Phys. Rev. Lett.* **119**, 180509 (2017).  
 [18] A. W. Harrow, A. Hassidim, and S. Lloyd, *Phys. Rev. Lett.* **103**, 150502 (2009).  
 [19] I. Kerenidis and A. Prakash, (2016), arXiv:1603.08675.  
 [20] D. C. McKay, C. J. Wood, S. Sheldon, J. M. Chow, and J. M. Gambetta, *Phys. Rev. A* **96**, 022330 (2017).  
 [21] K. M. Nakanishi, K. Fujii, and S. Todo, (2019), arXiv:1903.12166.  
 [22] R. Fletcher, *Practical Methods of Optimization* (John Wiley & Sons, 2013).  
 [23] R. H. Byrd, P. Lu, J. Nocedal, and C. Zhu, *SIAM J. Sci. Comput.* **16**, 1190 (1995).  
 [24] E. Jones, T. Oliphant, and P. Peterson, “SciPy: Open source scientific tools for Python,” (2001–).  
 [25] K. Temme, S. Bravyi, and J. M. Gambetta, *Phys. Rev. Lett.* **119**, 180509 (2017).

- [26] S. Endo, S. C. Benjamin, and Y. Li, Phys. Rev. X **8**, 031027 (2018).
- [27] Y. Li and S. C. Benjamin, Phys. Rev. X **7**, 021050 (2017).
- [28] P. J. OMalley, R. Babbush, I. D. Kivlichan, J. Romero, J. R. McClean, R. Barends, J. Kelly, P. Roushan, A. Tranter, N. Ding, *et al.*, Physical Review X **6**, 031007 (2016).
- [29] J. R. McClean, I. D. Kivlichan, K. J. Sung, D. S. Steiger, Y. Cao, C. Dai, E. S. Fried, C. Gidney, B. Gimby, P. Gokhale, *et al.*, arXiv preprint arXiv:1710.07629 (2017).
- [30] R. M. Parrish, L. A. Burns, D. G. A. Smith, A. C. Simmonett, A. E. DePrince, E. G. Hohenstein, U. Bozkaya, A. Y. Sokolov, R. Di Remigio, R. M. Richard, J. F. Gonthier, A. M. James, H. R. McAlexander, A. Kumar, M. Saitow, X. Wang, B. P. Pritchard, P. Verma, H. F. Schaefer, K. Patkowski, R. A. King, E. F. Valeev, F. A. Evangelista, J. M. Turney, T. D. Crawford, and C. D. Sherrill, J. Chem. Theory Comput. **13**, 3185 (2017).
- [31] J. Johansson, P. Nation, and F. Nori, Comput. Phys. Commun. **183**, 1760 (2012).
- [32] K. M. Nakanishi, “QuPy: A quantum circuit simulator for both cpu and gpu,” (2018–).

## Appendix A: Numerical SSVQE in SVQS procedures

### 1. Numerical SSVQE for single-qubit Rabi model

From the Fig. 13, one can see the formation of the energy subband caused by the magnetic field imposed on the ancilla qubit, and weighted-SSVQE can actually find desired excited states in the lowest energy sub-band all at once.

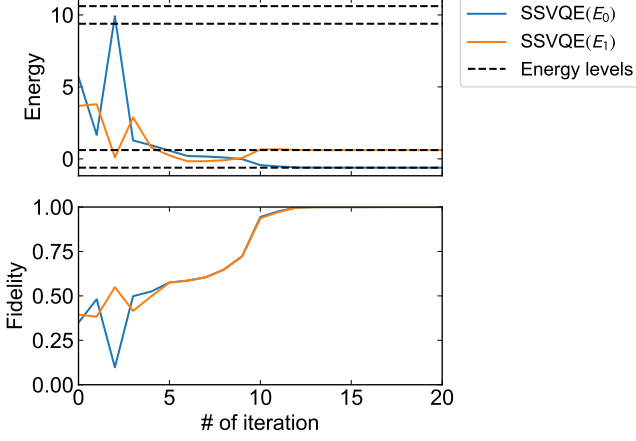


FIG. 13. The weighted SSVQE to find excited states of a transverse Ising model up to the third. In the energy diagram, SSVQE( $E_j$ ) (solid lines) are  $\langle \varphi_j | U^\dagger(\boldsymbol{\theta}) \mathcal{H}_{\text{total}} U(\boldsymbol{\theta}) | \varphi_j \rangle$  for each  $k$  at each iteration.

### 2. Numerical SSVQE for hydrogen molecular

From the Figs. 14 and 15, one can see weighted-SSVQE can actually find desired excited states in the lowest energy sub-band all at once.

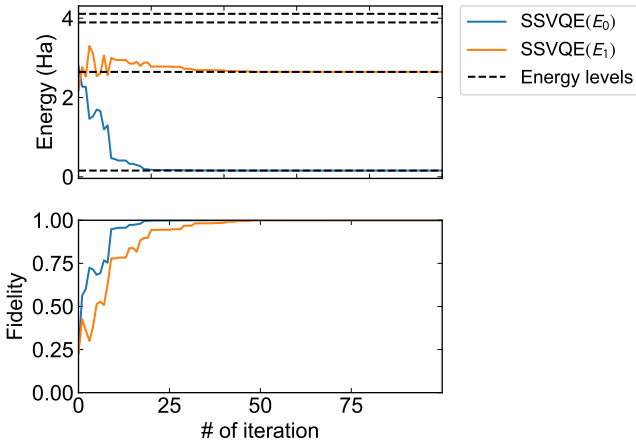


FIG. 14. The weighted SSVQE to find excited states of the hydrogen molecular with the interatomic distance  $0.2 \text{ \AA}$  up to the second. In the energy diagram, SSVQE( $E_j$ ) (solid lines) are  $\langle \varphi_j | U^\dagger(\boldsymbol{\theta}) \mathcal{H}_{\text{total}} U(\boldsymbol{\theta}) | \varphi_j \rangle$  for each  $k$  at each iteration.

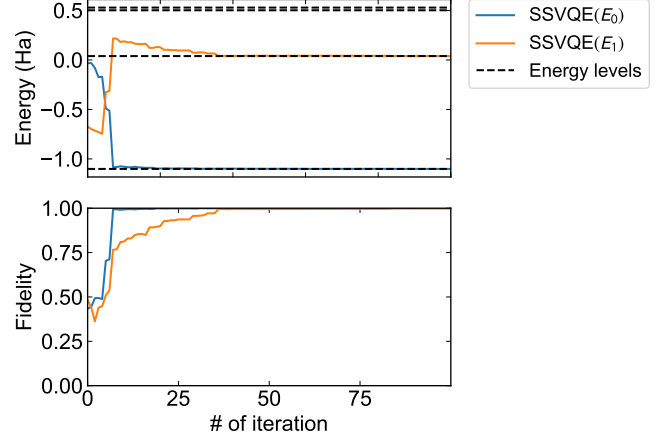


FIG. 15. The weighted SSVQE to find excited states of the hydrogen molecular with the interatomic distance  $1.0 \text{ \AA}$  up to the second. In the energy diagram, SSVQE( $E_j$ ) (solid lines) are  $\langle \varphi_j | U^\dagger(\boldsymbol{\theta}) \mathcal{H}_{\text{total}} U(\boldsymbol{\theta}) | \varphi_j \rangle$  for each  $k$  at each iteration.